

Spin-resolved photoemission from Ag(111): theory and experiment

E. Tamura¹, R. Feder¹, B. Vogt², B. Schmiedeskamp², and U. Heinzmann²

¹ Theoretische Festkörperphysik, Universität Duisburg-GH, Duisburg,
Federal Republic of Germany

² Universität Bielefeld, Fakultät für Physik, Bielefeld, Federal Republic of Germany

Received May 8, 1989

Using circularly polarized synchrotron radiation between 14 and 24 eV, spin-resolved normal photoemission spectra have been measured from an unreconstructed Ag(111) surface. Corresponding spectra were calculated by means of a fully relativistic one-step theory of photoemission together with the bulk band structures for real and complex potentials, using two different local approximations for the exchange-correlation potential. Experiment and theory employing an $X\alpha$ potential agree well with regard to existence and positions of peaks. Relative peak heights match except for an observed enhancement at photon energies, at which two or more direct interband transitions may “resonate”.

1. Introduction

Spin-resolved photoemission data, which had been obtained – using circularly polarized synchrotron radiation – for normal emission from (111) surfaces of Pt [1, 2], Ir [3] and Pd [4], were recently compared with theoretical results calculated by a fully relativistic one-step-model formalism [5]. For the real part of the initial-state effective potential, ground state potentials were employed, which had been calculated relativistically and self-consistently [6] using the Barth-Hedin [7] local exchange-correlation approximation. This led, for the three transition metals under study, to theoretical spectra, in which peak positions (i.e. initial state energies) agreed with experiment to within less than 0.3 eV and relative peak heights were reasonable (except for an observed resonant enhancement associated with a flat f -like final-state band).

In the present study, we extend the above spin-resolved photoemission work both experimentally and theoretically to the noble metal Ag. In Sects. 2 and 3, we address experimental and theoretical aspects, which are specific for this study. In Sect. 4, we present experimental and theoretical spectra for a range of photon energies and interpret them mostly in terms of direct transitions between bulk bands.

2. Experimental

The experiments were performed at the 6.5 m normal incidence monochromator at BESSY with normally incident circularly polarized light and for normal emission of the ejected photoelectrons. The overall energy resolution (electrons plus photons) was better than 150 meV at an angular resolution of $\pm 3^\circ$. The apparatus is in more detail described in [1]. In addition, evaporation facilities are now integrated, which allow to prepare thin Ag layers on Pt(111). A detailed description of the preparation and characterization procedure for the Ag layers is given in [8]. The Ag adsorbate layers turned out to grow epitaxially on Pt(111) and yielded for a coverage of 8 layers photoemission spectra, which were not different from those obtained in an earlier non-spin-resolved study for a Ag(111) single crystal [9]. All data presented in this work were obtained from this epitaxial 8 layer Ag adsorbate.

3. Theory

Let us first recall that general properties of the spin polarization vector \mathbf{P} of the photocurrent can be ob-

tained, without numerical calculations, by symmetry considerations in the one-step model (Ref. 5 and references therein). For circularly polarized radiation incident and electrons emitted normally to an fcc(111) surface, \mathbf{P} is parallel or antiparallel to the surface normal. Its component P is +1 and -1 (i.e. $\pm 100\%$ polarization) for transitions from initial states of A_{4+5} and A_6 symmetry, respectively, into final states with A_6^1 symmetry (for light of positive helicity incident on the surface).

Our relativistic one-step model theory has been presented in detail [10, 11] and briefly reviewed [5]. It remains to specify an effective quasi-particle potential for the present case of Ag.

For the (spherically symmetric) ion-core scattering part, our previous results for Pt, Ir and especially Pd (which has only one electron per atom less than Ag) suggest as a first choice a self-consistent ground state potential obtained by the scalar relativistic LMTO-ASA method using the local exchange-correlation approximation of Barth and Hedin [6, 7]. We recall that for non-magnetic systems this exchange-correlation approximation coincides with the one due to Hedin and Lundquist [12]. Since this type of potential was found to produce rather high-lying d -bands for Ag [13], we employ as a second choice a relativistic self-consistent potential based on the $X\alpha$ local exchange approximation with $\alpha=0.82$ chosen to fit photoemission data [14]. The real part of the uniform inner potential for the initial state is taken as $(\phi + E_F)$, which with work function $\phi=4.7$ eV gives 11.8 eV for the first and 11.2 eV for the second potential. For the final states we firstly use the same values and secondly values reduced by 1 eV “self-energy correction” (as discussed in [5]). The imaginary part of the initial state self-energy is chosen to rise linearly as $0.1(E - E_F)$ eV with the distance from E_F . The rather large values, between 0.4 and 0.7 eV, in the d -band region are intended to mimic simultaneously the experimental energy resolution. For the imaginary part of the final state self-energy we use the form $a(E - E_F)^b$ (eV) [15] with $a=0.04$ and $b=1.2$. On the grounds of a LEED analysis [16], the surface geometry is assumed as unreconstructed (i.e. in particular without a displacement of the topmost layer).

4. Results and discussion

As a basis for the interpretation of our photoemission spectra, we show in Fig. 1 the relativistic bulk band structures, which we obtained (via diagonalization of the layer transfer matrix) from the two above-described ion-core potentials. They are seen to differ strongly from each other below E_F . For the $X\alpha$ po-

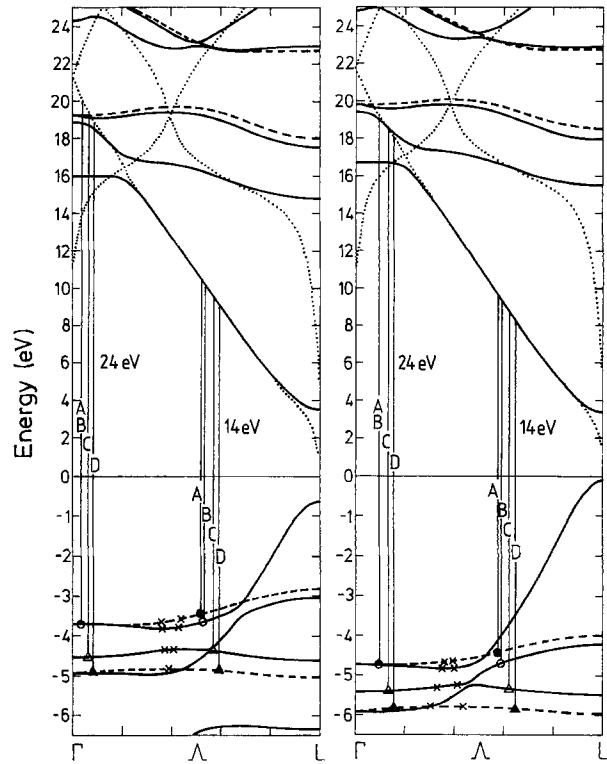


Fig. 1. Relativistic bulk band structure of Ag along $\Gamma(A)L$ with symmetry types A_6 (—) and A_{4+5} (---) obtained from real potentials due to Christensen [6] (left-hand panel) and Eckardt et al. [14] (right-hand panel) and modification of final-state bands by the imaginary part of self-energy V_2 (.....). The energy 0 is the Fermi level. The vertical lines point out direct transitions at photon energies as indicated. (Note the reduction of the energy scale above E_F relative to the one below)

tential (right-hand panel), the d -bands are somewhat narrower and lowered by about 1 eV. As was discussed in [13], such lowering reduces the $sp-d$ hybridization towards E_F and thereby raises the sp -like band near L . Consequently, the “ L gap” is reduced by about 0.5 eV. Comparing with earlier results, we note that our “Christensen band structure” (left-hand panel) is practically identical with the one shown in [13]. Our right-hand band structure, while necessarily identical with the one in [14] (whose potential we used), turns out to be fairly close to an early non-self-consistent RAPW band structure obtained by Christensen [6] from an atomic-overlapping potential with Slater’s exchange approximation ($\alpha=1$, as compared to 0.82 in the potential in [14]).

Theoretical spin-resolved photoemission spectra obtained from the two potentials for photon energies 14 and 24 eV are shown in Figs. 2 and 3. For each initial state symmetry, they exhibit a large peak (A for A_{4+5} and B for A_6) and a small one (D and C). Without a real self-energy correction ΔV_r (dashed

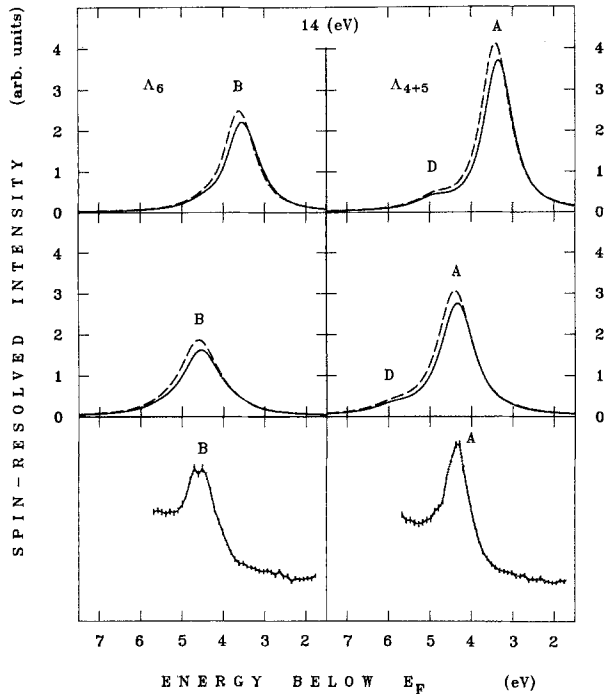


Fig. 2. Normal photoemission from Ag(111) by normally incident circularly polarized radiation of energy 14 eV. The left (right) column shows partial intensity spectra $I_-(I_+)$ arising from $\Lambda_6(\Lambda_{4+5})$ initial states. The upper two rows give theoretical spectra obtained using real potential parts due to Christensen (1987) (1st row) and Noffke and Fritsche (1984) (2nd row) with (—) and without (---) a real self-energy correction of 1 eV to the upper-state potential. The third row gives the corresponding experimental spectra. The error bars show the total error including the statistical errors of the count rates and the uncertainty of light polarization and detector asymmetry function

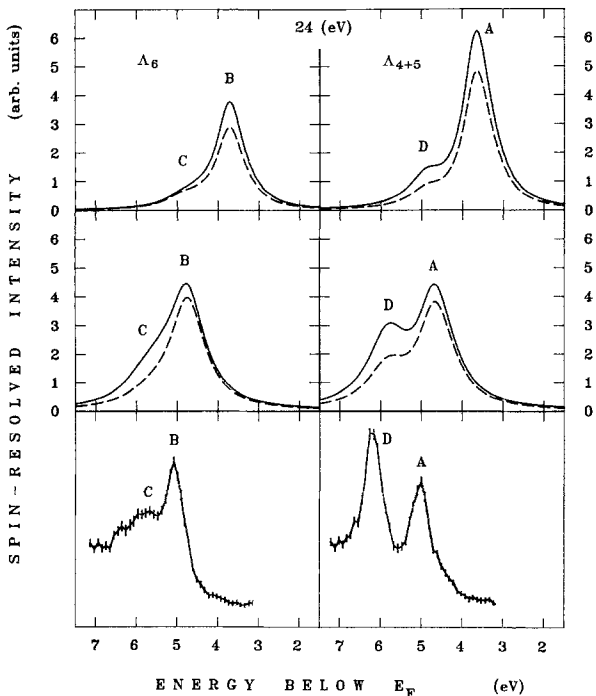


Fig. 3. As Fig. 2, but for photon energy 24 eV

lines), these peaks are identified as due to the bulk interband transition indicated by vertical lines in the band structure of Fig. 1. With $\Delta V_r = 1$ eV, which implies a raising of the final state bands by 1 eV, A and B at $\hbar\omega = 14$ eV shift to the right by about 0.2 eV, whereas at $\hbar\omega = 24$ eV there is no shift because of the flatness of the initial state bands near the Γ point.

Comparison with the experimental spectra for $\hbar = 14$ eV (bottom panels in Fig. 2) shows excellent agreement with the theoretical spectra from the $X\alpha$ potential, whilst those from the Hedin-Lundquist potential are displaced by about 1 eV towards E_F . For $\hbar\omega = 24$ eV (Fig. 3), peaks A to D in the experimental spectra occur at energies about 0.3 eV lower than in the $X\alpha$ -potential theoretical spectra and about 1.3 eV lower than in the Hedin-Lundquist-potential spectra. This clearly demonstrates that the latter potential is not appropriate, while the $X\alpha$ potential, for which $\alpha = 0.82$ had been chosen to fit earlier not spin-resolved photoemission data, is reasonable for the present data. Increasing α to the Slater value $\alpha = 1$ would shift peaks somewhat to the left, thereby improving the agreement at 24 eV but worsening it at 14 eV. The strong enhancement of the experimental peak D in Fig. 3 relative to the experimental peak A and to the theoretical peak D is a phenomenon already found for Pd, Ir and Pt [5]. It is associated with a final state energy near a flat f -like band, as can be seen in the $X\alpha$ band structure (right panel in Fig. 1) after raising the upper bands by about 1 eV self-energy correction. In addition to the 24 eV transition marked by a vertical line, the crossing final state bands (for complex potential, dotted lines in Fig. 1) can be reached at a nearby k and resonance between the two transitions may take place.

For photon energies between 14 and 24 eV, experimental spectra are shown in Fig. 4 together with their theoretical counterparts as obtained from the $X\alpha$ potential. For $\hbar\omega = 16$ and 18 eV, agreement between experiment and theory is excellent as for 14 eV except for some excess of the theoretical A/B height ratio over the experimental one. The slight left-shift of the positions of A and B with increasing photon energy is a consequence of the dispersion of initial state bands, from which transitions occur into the sp -like final state band (cf. Fig. 1). For $\hbar\omega = 20$ eV, the experimental spectra exhibit, in contrast to the theoretical ones, already appreciable peaks C and D . These become even stronger for $\hbar\omega = 20$ eV. Comparing with data for $\hbar\omega = 21$ and 23 eV (not shown), peak C is maximal for 22 eV and D for 23 eV. Further, for $\hbar\omega = 22$ eV, the experimental peaks A and B are seen to be strongly reduced. These anomalies were also found in earlier non-spin-resolved measurements (cf. Figs. 15 and 16 in [9]).

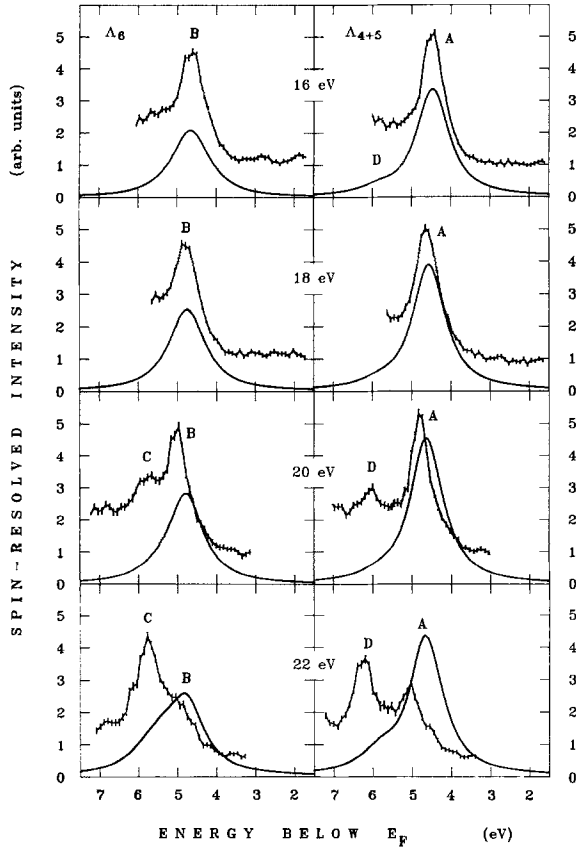


Fig. 4. Experimental (+++++) and theoretical normal photoemission spectra due to normally incident circularly polarized photons of energies from 16 to 22 eV as indicated in each row

In search for an explanation, one might first think of details of the exchange-correlation approximation, as suggested by Fig. 3, where the intensity of D for the $X\alpha$ -potential is by a factor of 3 larger than for the Hedin-Lundquist potential. Since it is still much smaller than the experimental intensity and since a stronger modification of the potential would lead to larger discrepancies in peak positions, we feel, however, that this is a relatively minor contributing factor and that the main reason lies elsewhere.

In Ref. 9, three-step-model results according to [17], which combine bulk interband transition matrix elements with a surface transmission factor, were shown to produce the C and D peak enhancement observed for s -polarized light almost quantitatively, with final states lying in the flat region of the first unoccupied Λ_6 band near Γ . Applying this model in the case of p -polarized light, for which the experimental data are similar (cf. Fig. 16 in [9]), we find, however, that it cannot even qualitatively explain the data. Also, it fails to explain findings in recent spin-resolved photoemission experiments [8]. Our conclusion, that

the relevant physical mechanism is not taken into account and that the agreement for the s -polarized case is accidental, is further supported by the following arguments. Firstly, in the framework of the three-step-model, the appropriate final state bands are the ones obtained for a complex potential, i.e. the dotted lines in Fig. 1 rather than the solid ones. While the difference between the two is negligible in the steep s - p -like band, it becomes crucial in the region of hybridization with the flat f -line band. Secondly, the three-step model is an approximation to our present one-step model and does certainly not contain extra physical mechanisms. Features of three-step model results, which reproduce experimental features, should therefore a fortiori be present in one-step model results. Faith in our relativistic formalism and computer code is strengthened by the level of agreement for Pd(111) [5] with earlier independent non-relativistic calculations [18]. In particular, both failed to produce the experimentally observed intensity “resonances”.

We therefore conclude that their origin should be a physical mechanism not contained in present-day one-step-model theories. A clue to this mechanism is that all the above observed anomalies occur at photon energies such that the final state energies are in the region of hybridization with the flat f -like band. Focusing on peaks C and D , our band structure (right-hand panel of Fig. 1) shows that e.g. for $\hbar\omega = 20$ eV three transitions are possible into the three complex-potential final state bands (dotted lines), of which two are fairly close to each other in k . The ensuing resonant enhancement gets stronger with decreasing k separation, as is demonstrated by the experimental spectra for $\hbar\omega = 22$ eV in Fig. 4. The photon energies, for which the experimental intensities are maximal, are those, for which the two final states on the dotted bands are closest to the crossing point. We conclude that the physical origin of the enhancement of peaks C and D as well as of the reduction of A and B is resonance between competing direct transitions.

5. Conclusion

The present experimental spin-resolved photoemission spectra are quite closely reproduced by relativistic one-step-model calculations employing a potential with an $X\alpha$ exchange approximation with $\alpha = 0.82$, whilst spectra calculated with the Hedin-Lundquist exchange correlation potential are shifted towards smaller binding energies by about 1 eV, which implies a corresponding shift of the quasi-hole initial states. This finding is in accordance with earlier

work involving non-spin-resolved photoemission (cf. [9] and references therein). In search of an explanation, it was suggested [13, 19] that, while Hedin-Lundquist exchange was appropriate for ground state properties, the much stronger Slater exchange form (i.e. $X\alpha$ with $\alpha=1$) simulated a quasi-particle self-energy correction. If this is so, the adequacy of the Hedin-Lundquist form found in our recent study for Ir, Pt and Pd [5] implies that self-energy corrections are small for these transition metals with one or two d holes, whilst they are strong (about 1 eV real-energy shift) for the noble metal Ag with its closed d shell. An alternative or at least contributing origin of this difference might be that the local density approximation to the exchange-correlation potential is less adequate for noble metals, since their d electrons are more tightly bound. Further, one has to bear in mind that the Fermi energy for noble metals lies in an sp -band energy range with a density of states, which is far smaller than in the d -band region. Errors inherent in the local-density approximation and in the underlying homogeneous electron gas results (e.g. the Random Phase Approximation in the Hedin-Lundquist case) can therefore be expected to have a much stronger effect on the calculated position of the Fermi energy.

For photon energies such that final states are, in the real-potential band structure, in the hybridization gap between an sp -like band and a flat f -like band or, more appropriately speaking, on two complex-potential-derived bands near their crossing point, the present experimental spectra for Ag exhibit – like previous spectra for Pt, Ir and Pd – strong peaks, which are absent in the calculated spectra. The mechanism of this enhancement is probably resonance between two or more competing direct transitions.

In conclusion, the present study demonstrates the power of spin-resolved photoemission. Substantial agreement has been achieved between experiment and theory. Remaining discrepancies point to the need for more fundamental theoretical work on the “potential problem” and for incorporating “resonance mechanisms” into our relativistic photoemission theory.

This work was funded by the German Federal Ministry for Research and Technology under Contracts No. 05336CAB9. and No. 05331AX. Our gratitude extends to H. Gollisch for useful discussions and to N.E. Christensen and J. Noffke for supplying us with their Ag potentials. Also, we are pleased to acknowledge the cooperative hospitality of the Institut für Festkörperforschung of the KFA Jülich, of the Fritz-Haber-Institut of the MPG, and of BESSY.

References

1. Eyers, A., Schäfers, F., Schönhense, G., Heinzmann, U., Oepen, H.P., Hünlich, K., Kirschner, J., Borstel, G.: Phys. Rev. Lett. **52**, 1559 (1984)
2. Oepen, H.P., Hünlich, K., Kirschner, J., Eyers, A., Schäfer, F., Schönhense, G., Heinzmann, U.: Phys. Rev. B **31**, 6846 (1985)
3. Müller, N., Kessler, B., Schmiedeskamp, B., Schönhense, G., Heinzmann, U.: Solid State Commun. **31**, 6846 (1987)
4. Schmiedeskamp, B., Kessler, B., Müller, N., Schönhense, G., Heinzmann, U.: Solid State Commun. **65**, 665 (1988)
5. Tamura, E., Piepke, W., Feder, R.: J. Phys.: Cond. Matter (1989)
6. Christensen, N.E.: Private communication (1987)
7. Barth, U., Hedin, L.: J. Phys. C **5**, 1629 (1972)
8. Schmiedeskamp, B., Kessler, B., Vogt, B., Heinzmann, U.: (to be published)
9. Wern, H., Courths, R., Leschick, G., Hüfner, S.: Z. Phys. B – Condensed Matter **60**, 293 (1985)
10. Ackermann, B., Feder, R.: J. Phys. C **18**, 1093 (1985)
11. Ackermann, B., Feder, R.: Solid State Commun. **54**, 1077 (1985)
12. Hedin, L., Lundquist, B.I.: J. Phys. C **4**, 28 (1971)
13. Jepsen, O., Glötzel, D., Mackintosh, A.R.: Phys. Rev. B **23**, 2684 (1981)
14. Eckardt, H., Fritsche, L., Noffke, J.: J. Phys. F **14**, 97 (1984)
15. McRae, E.G., Caldwell, C.W.: Surf. Sci. **57**, 77 (1976)
16. Soria, F., Sacedon, J.L.: Surf. Sci. **68**, 448 (1977)
17. Benbow, R.L., Smith, N.V.: Phys. Rev. B **27**, 3144 (1983)
18. Hora, R., Scheffler, M.: Phys. Rev. B **29**, 692 (1984)
19. MacDonald, A.H., Daams, J.M., Vosko, S.H., Koelling, D.D.: Phys. Rev. B **25**, 713 (1982)

E. Tamura, R. Feder
Theoretische Festkörperphysik
Universität Duisburg-GSH
Postfach 10 1629
D-4100 Duisburg 1
Federal Republic of Germany

B. Vogt, B. Schmiedeskamp, U. Heinzmann
Fakultät für Physik
Universität Bielefeld
Universitätsstrasse
Postfach 8440
D-4800 Bielefeld 1
Federal Republic of Germany